Wilfred Chinedu Okologume,*
Omonigho Famous Ovuakporaye

Department of Petroleum Engineering, Federal University of Petroleum Resources, Effurun, Delta state Nigeria

Scientificpaper
ISSN 0351-9465, E-ISSN 2466-2585
https://doi.org/10.62638/ZasMat1792

Zastita Materijala 67 ()
(2026)

Adsorption capacity of african pear seed (*Dacryodes edulis*) derived-activated carbon for sulfidic gases' capture

ABSTRACT

This study investigates the adsorption capacity of activated carbon derived from African pear (Dacryodes edulis) seeds for the capture of sulfidic gases. Activated carbon was prepared through chemical activation by adding NaOH and characterized in terms ofBrunauer–Emmett–Teller (BET) surface area analysis, Fourier transform infrared (FTIR) spectroscopy, Scanning electron microscopy (SEM), Energy dispersive x-ray (EDX) spectroscopy, and X-ray diffraction (XRD)techniquesmethods of activated carbon before and after gas adsorption. Experiments in adsorption were performed on the fixed-bed system with temperatures of 25°C and 50°C under pressure between 5 and 20 psi. The analysis of the surface area revealed that the surface area changed to 965.2 m ^{2}/g to 999.9 m ^{2}/g, whereas the average pore diameter changed to 2.40 nm to 3.00 nm, indicating that the restructuring of the pores slightly occurred following the interaction with gases. FTIR analysis indicated that sulfur containing functional groups were formed during the adsorption process and SEM micrographs indicated morphological changes and partial pore coverage. The XRD patterns proved the existence of crystalline sulfur-related species on the carbon surface. Pressure increased the adsorption capacity to a maximum of 2.96mmol/g at 25°C and 2.16 mmol/g at 50°C. The isotherm analysis showed that temperature dependence was best characterized by Temkin and Freundlich models indicating that the adsorption behaviour was heterogeneous adsorption on the surface and adsorbate-adsorbent interactions. The statistical analysis also showed that the adsorption capacity was greater at lower temperature, which means that the adsorption behaviour was temperature dependent. The findings indicate that African pear seed-obtained activated carbon is a potential sustainable low-priced adsorbent of sulfidic gases in industrial gas streams.

***Keywords**: African Pear, Adsorption,Capture, Gas, Sulfur, Activated carbon*

1. INTRODUCTION

Sulfur-bearing acid gases, particularly hydrogen sulfide (H_2S) and sulfur dioxide (SO_2), remain persistent contaminants in refinery vents, natural-gas conditioning systems, anaerobic-digester off-gas, and industrial odour-control streams [1]. Even at low concentrations, these gases accelerate corrosion, poison catalysts, and negatively impact operational reliability. This explains why many facilities continue to rely on fixed-bed polishing units, which can operate at ambient temperature with low pressure drop while delivering deep removal of residual sulfur species.

Activated carbons remain attractive because they combine adsorption capacity, operational simplicity, and economic viability relative to competing technologies [2,3].

The performance of activated carbon in sulfidic environments is governed by both ultra-micropore physisorption and surfacemediated reactions promoted by moisture, oxygen, and redox-active sites. Targeted activation and impregnation strategies can enhance uptake and extend service life, but performance varies widely with precursor choice, pore architecture, and surface chemistry. This variability has intensified interest in biomass-derived carbons, which offer low-cost feedstocks and tunable structures through chemical activation.

Across West and Central Africa, African pear, locally known in Nigeria as "ube" and botanically *Dacryodes edulis* (Burseraceae), offers a particularly promising precursor stream. The fruit is

*Corresponding author: Wilfred Chinedu Okologume
E-mail: okologume.wilfred@fupre.edu.ng
Paper received: 16.02.2026.
Paper accepted: 27.03,2026.

widely consumed; the pulp supports regional food systems, and the seed is frequently discarded at scale, which provides a dependable feedstock for valorization. Botanical and ethnobotanical surveys describe the distribution, processing, and composition of the species, reinforcing its suitability as a carbon-rich, lignocellulosic waste for sorbent manufacture in a circular-economy model [4,5,6].

Industrial and municipal systems that handle sour gas streams continue to face operational and environmental challenges from hydrogen sulfide and sulfur dioxide. While activated-carbon polishing beds are widely used, their effectiveness depends strongly on pore structure, surface chemistry, humidity, and oxygen availability.

Despite the abundance of African pear seed waste in Nigeria and neighboring regions, there is limited quantitative evidence on its performance as a precursor for activated carbon targeting sulfidic gases. Furthermore, structure-function relation ships, promoter effects, and regeneration stability for ube-seed carbons remain insufficiently mapped. without this information, it is not possible to deter-mine whether locally produced ube-seed activated carbon can match or exceed commercial materials in adsorption capacity, durability, and operational practicality. This gap constrains both technological adoption and technoeconomic assessment.

This research addresses a combined technical and regional resource challenge. By evaluating activated carbon derived from *Dacryodes edulis* seeds for hydrogen sulfide and sulfur dioxide capture, the study will generate foundational data linking activation chemistry, pore structure, and surface functionality to gas-phase adsorption performance.

2. MATERIALS AND METHODS

2.1. Materials, Chemicals and Apparatus

The precursor materials, African pear seeds, were sourced from Agbarho markets in Delta State, Nigeria. Distilled water was obtained from the laboratory, and sodium hydroxide (NaOH) was procured from Wintek Chemicals, a Sigma Aldrich product. The apparatus and instruments used included a muffle furnace, oven, pH meter, electronic digital weighing balance,Brunauer-Emmett-Teller(BET) analyzer, Fourier Transform Infrared (FTIR) spectrometer, Scanning Electron Microscopy (SEM), X-ray Diffraction (XRD), Energy-dispersive X-ray (EDX), grinding machine, cylindrical glass beaker, and batch adsorption setup.

2.2. Methods

The methods comprised the preparation of activated carbon from African pear seeds, characterization of the resulting material, batch adsorption tests for H_2S and SO_2, and pH and proximate analyses of the activated carbon.

The selected African pear seeds were pre-treated to remove impurities and reduce moisture. They were thoroughly washed with clean tap water to eliminate dirt, sand, and adhering organic residues, followed by a final rinse with distilled water to remove soluble salts or contaminants. After washing, the samples were sun-dried for 2 weeks. The dried material was carbonized in a furnace under limited oxygen conditions to convert the biomass to char. Following the method by Sumathi and Alagumuthu [7], carbonization was conducted in a muffle furnace at 500°C for 2 hours to optimize char yield without complete combustion. The reactor was sealed to minimize oxygen influx and ensure pyrolytic conditions. After carbonization, the char was allowed to cool to room temperature in a desiccator to avoid oxidation, then ground with a mechanical grinder to reduce particle size and increase surface area and sieved to obtain a uniform particle size for consistent heat and chemical penetration. Chemical activation was carried out by mixing the carbonized biochar with 0.5 M NaOH; the mixture was stirred for 4 hours at 70°C to promote deep penetration of the activating agent, after which the sample was oven-dried at 10°C for 24 hours for activation. Following activation, the product was repeatedly washed with warm distilled water until the pH approached neutrality to remove residual activating agents and soluble impurities. Finally, the washed material was oven-dried at 105°C for 24 hours to remove moisture, then cooled, ground, and sieved to obtain the activated carbon for subsequent instrumental characterization.

2.2.1. Characterization of the African pear seeds Activated Carbon

To evaluate the physicochemical properties of the activated carbon produced from agricultural waste, the following characterization techniques were employed.

The BET method was used to determine the specific surface area, total pore volume, and average pore diameter of the activated carbon. Nitrogen adsorption–desorption isotherms were obtained at 77 K using a BET surface analyzer. Before analysis, the activated carbon samples were degassed under vacuum at 200°C for 4 hours to remove moisture and contaminants. BET analysis provides insight into the material's porosity, a key determinant of adsorption performance. This analysis is essential to determine whether the activated carbon is microporous (<2 nm), mesoporous (2-50 nm), or macroporous (>50 nm), as these structures influence its application potential.

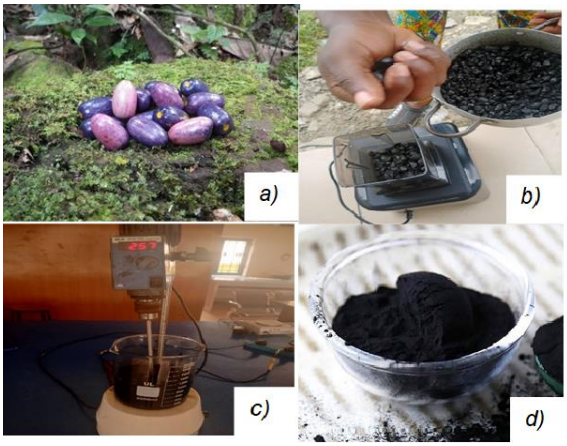

Figure 1. The Activated carbon preparation process, (a) African Pear sample, (b) grounding of carbonized African pear seed, (c) activation of carbonised African pear seed (d) activated African Pear seed carbon.

The FTIR spectroscopy was performed to identify the functional groups on the surface of the activated carbon. The activated carbon sample would be mixed with potassium bromide (KBr) and pressed into a transparent pellet. The FTIR spectrum would be recorded over a wavenumber range of 4000 - 400 cm^{-1}. The FTIR spectrum shows peaks corresponding to hydroxyl (-OH), carbonyl (C=O), carboxyl (-COOH), alkene (C=C), and aromatic groups, all of which play vital roles in contaminant adsorption.

SEM was carried out to examine the surface texture and morphology of the activated carbon. A small amount of powdered sample was mounted on an aluminium stub using conductive adhesive. The sample would be coated with a thin layer of gold or carbon to enhance conductivity. SEM images were captured at various magnifications to observe the porous structure, surface cracks, and particle distribution. SEM provides visual confirmation of pore formation and surface roughness, which are critical for adsorption activity [8].

EDXSpectroscopy, usually coupled with SEM, was used to determine the elemental composition of the activated carbon. The EDX detector collects X-rays emitted from the sample during SEM imaging.

XRD analysis was conducted to determine the crystallinity or amorphous nature of the activated carbon. The sample was analyzed using an X-ray diffractometer with Cu-Kα radiation (λ = 1.5406 Å). Scans were conducted over a 2θ range of 10° to 80° at a scan rate of 2°/min. Activated carbon typically shows broad peaks around 2θ = 20°- 30°, indicating amorphous carbonaceous structure. Any sharp peaks would signify the presence of crystalline impurities or mineral residues.

The pH of the activated carbon was determined using a pH meter to assess its surface acidity or basicity, which is believed to influence its adsorption behaviour, as described by [1]. This was performed using the slurry method. 1g sample of activated carbon was added to 100 mL of distilled water in a 100 mL beaker and stirred continuously for 30 minutes. The suspension was allowed to stand for another 30 minutes to stabilize. The pH of the supernatant was measured using a digital pH meter.

Proximate analysis was done to determine moisture content, ash content, volatile matter, and fixed carbon using procedures described by [1].

For Moisture content determination, 2g of the activated carbon was weighed and placed in crucibles. The sample was then dried in an-air oven at 105°C for 12 hours until a constant weight was achieved. After cooling in a desiccator, the final weight was recorded. (Eq. 1) was used to calculate the moisture content of the activated carbons.

$$Moisture\ Content\ (\%) = \frac{W_1 - W_2}{W_1} \times 100 \quad (1)$$

Where:

W_1 -Initial weight of sample (g)

W_2 - Weight after drying (g)

For Ash content determination, 2g weight of the activated carbons samples were placed in a clean crucible and incinerated in a muffle furnace at 600°C for 3 hours. The crucible was cooled in a desiccator and reweighed. The (Eq. 2) below was used to calculate the ash content.

$$Ash\ Content\ (\%) = \frac{W_1}{W_2} \times 100 \quad (2)$$

Where

W_1 - Initial weight of dry sample (g)

W_2 - Weight of ash residue (g)

To estimate volatile matter, about 2g of the dried sample was placed in a covered crucible and heated at 950°C for 7 minutes in a muffle furnace to avoid oxidation. The crucible was cooled in a desiccator and reweighed. (Eq. 3) was used to calculate the fixed carbon of the activated carbons.

$$Volatile\ Matter\ (\%) = \frac{W_1 - W_2}{W_s} \times 100 \quad (3)$$

W_1 - Initial weight of sample plus crucible (g)

W_2 -Weight of residue after heating plus crucible (g)

$W_s = W_1 - W_{crucible}$ (g)

Fixed carbon content was calculated by subtracting the sum of moisture content, ash

content, and volatile matter from 100%. (Eq. 4) was used to calculate the fixed carbon of the activated carbons.

$$Fixed\ Carbon = 100 - (Moisture +) \\ +Ash + Volatile\ Matter) \quad (4)$$

2.2.2. Batch adsorption experiments

In the adsorption experiments, single-component sulfidic gases, H_2S and SO_2, were used and supplied in high-purity compressed gas cylinders. The activated carbon adsorption was tested under controlled laboratory conditions by loading each gas separately into the adsorption column. The experiments were conducted at 25 °C and 50 °C, and at pressures of 5 psi, 10 psi, 15 psi, and 20 psi; the gas flow rate was kept at about 100 mL/min using a pressure regulator and needle valve. The adsorption experiments were conducted with the fixed-bed adsorption system, as shown in Figures 2 and 3. The adsorption column was a laboratory-scale cylindrical glass reactor with an internal diameter of 2.0 cm and a bed height of about 10 cm.

Firstly, the vacuum pump (VP) was used to remove air and stray gas molecules from the air-tight apparatus, ensuring that no other gases were present in the system before the adsorption process. Thereafter, the Dosing Valve (DV) and Bleeding Valve (BV) were shut, while the Inlet Valve (IV) was opened for gas passage. The prepared African pear seed-derived activated carbon was ground to a measured mass of 0.5g and loaded into the column (Figure 2b), which was supported between two layers of quartz wool to ensure uniform gas distribution and prevent loss of adsorbent particles. Then, gas flowed into the staging manifold from a gas cylinder while the DV and BV were closed. This allowed pressure to build to target levels of 5, 10, 15, and 20 psi, using a stopwatch. After that, the gauge was quickly closed to maintain constant pressure. After which, the gauge was quickly shut in to maintain constant pressure. Afterwards, equilibration temperature was attained for 30 minutes and DV was carefully opened so that gas can flow into the reactor that was immersed in a water bath (WB) which contain the activated carbon, it was kept constant at an ambient temperature of 25°C and 50°C, allowing the sulfidic gas stream to come into contact with adsorbent for adsorption process to occur. Consequently, the adsorption capacity of the activated carbon was then calculated.

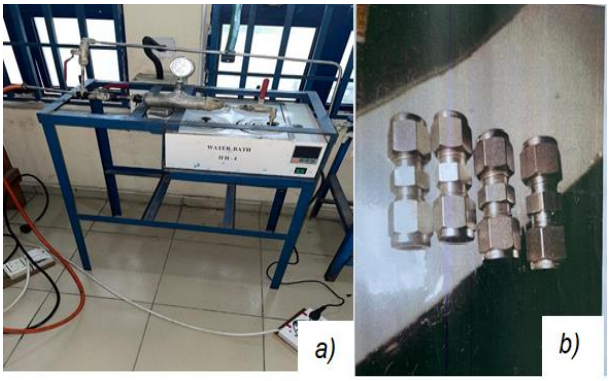

Figure 2. H_2S and SO_2 adsorption equipment, (a)Experimental setup for evaluation of H_2S and SO_2 adsorption capacity (b) Reactors for storing adsorbents

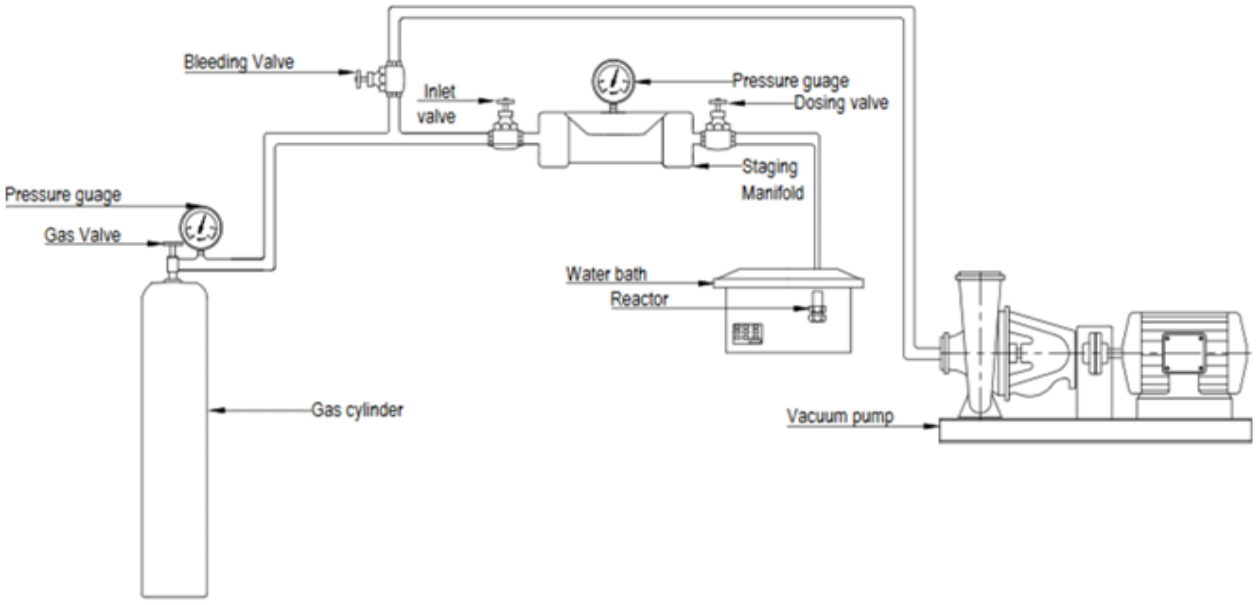

Figure 3. Schematic of H_2S and SO_2 adsorption experimental setup

3. RESULTS AND DISCUSSION

3.1. African pear seed activated carbon characterization result for before and after H_2S and SO_2 gas capture.

The FTIR spectrum of activated carbon from African pear seed before and after gas capture is presented in Figure 4 and 5, respectively. Before adsorption, the FTIR spectrum displayed prominent peaks around 3400 cm^{-1}, corresponding to –OH stretching vibrations from hydroxyl groups. These groups are known to enhance the polarity of the carbon surface, thereby facilitating interactions with polar gas molecules such as hydrogen sulfide (H_2S). Additionally, peaks near 1600 cm^{-1} and 1400 cm^{-1} were linked to aromatic C=C stretching and O–H bending, respectively, further confirming the presence of reactive sites [9].

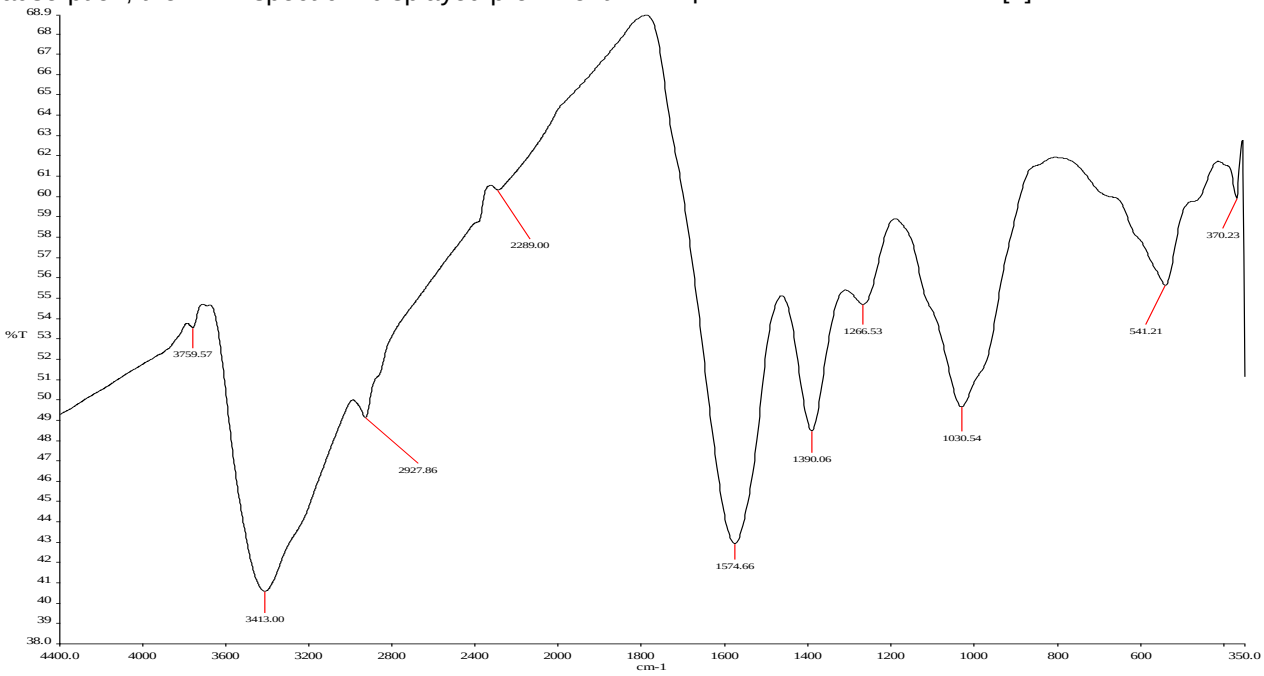

Figure 4. FTIR spectra of activated carbons from African pear seed before adsorption.

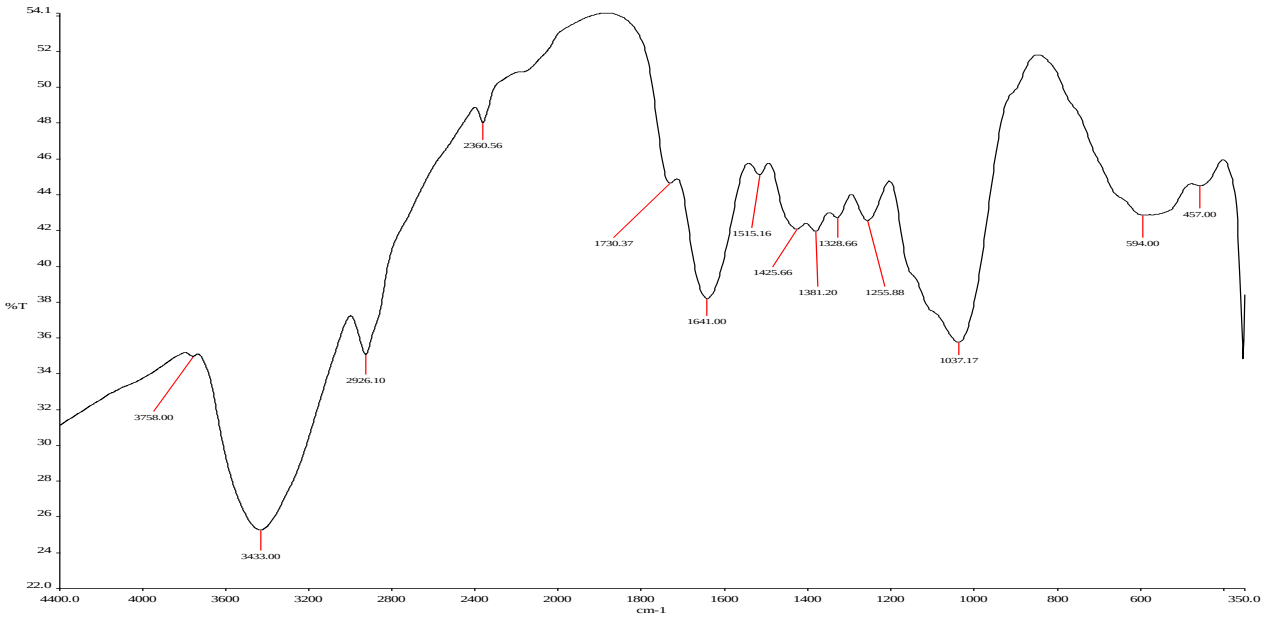

Figure 5. FTIR spectra of activated carbons from African pear seed after adsorption

After adsorption, the FTIR spectrum showed a reduction in the intensity of the –OH and C=O peaks, suggesting that these groups were involved in binding sulfidic gas molecules. A new peak emerged near 1328.66 cm^{-1}, which correspond to S=O stretching vibrations, indicating the presence

of adsorbed sulfur species. This shift supports the hypothesis that sulfidic gases were chemically adsorbed onto the carbon surface [10]. These changes in the fingerprint region of the spectrum are consistent with FTIR studies of activated carbon used for biogas desulfurization, where sulfur-containing gases alter the surface chemistry upon adsorption [11].

EDX spectra ofthefixed carbonof activated carbon from African pear seed before and after gas capture is presented in Figure 6. The result of the Energy Dispersive X-ray Spectroscopy (EDS) showed that there was a great increase in the content of sulfur, carbon and oxygen after adsorption, which showed that acid gases were captured successfully. This correlates with more recent results that waste-based activated carbons made out of agricultural wastes have a high adsorption potential as they have a porous structure and surface chemistry [12].

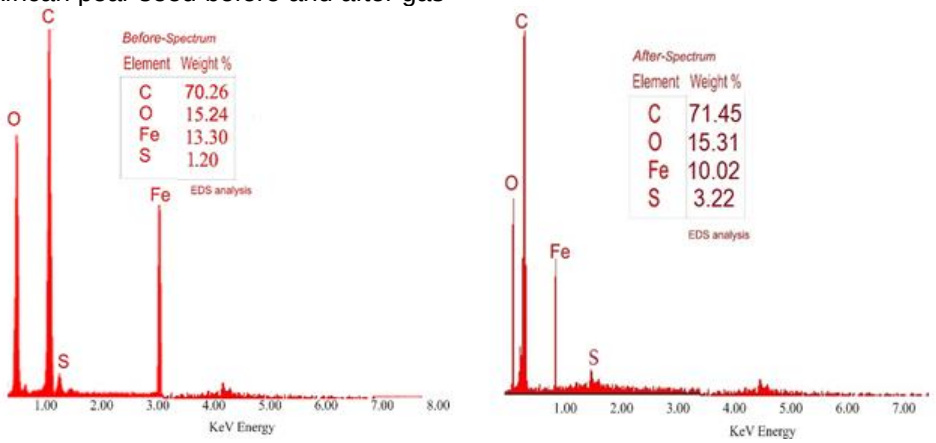

a) *b)*

Figure 6: EDX spectra of activated carbon from African pear seed before (6a) and after adsorption (6b)

In the elemental composition, prior to adsorption, carbon was (70.26 wt%), sulfur was (1.20 wt%), oxygen was (15.24 wt%) and iron was (13.3 wt%). Carbon increased after reaction to (71.45 wt%), sulfur was (3.22 wt%), oxygen was increased to (15.31 wt%) and iron was reduced to (10.02 wt%). The Increase in sulfur and carbon and oxygen indicates adsorption of sulfidic gases (e.g hydrogen sulfide, H_2S or sulfur oxides, SO_x, where x could be 2 or 1) and adsorption of other organic and oxidizing species respectively. These changes are aligned with the new EDX-based research that has shown the capacity of activated carbon to trap acid gases, either in the physisorption or chemisorption process [13].

The SEM micrographs (SEM) of activated carbon from African pear seed provides critical insights into the surface morphology of adsorbents as presented inFigure 7. which directly influences their adsorption capacity. SEM micrographs of activated carbon derived from African pear seeds were analyzed before and after exposure to sulfidic gas. The “Before” micrograph revealed a rough, irregular surface with densely packed particles, indicative of a high surface area and porous structure key attributes for effective gas adsorption [8].

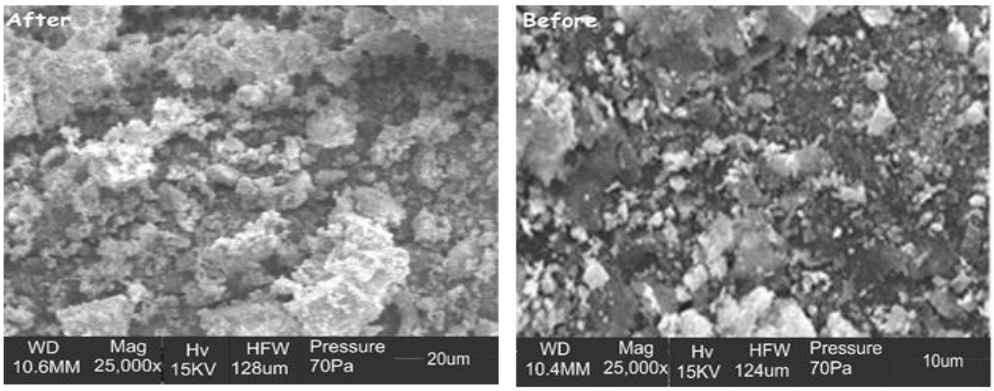

a) *b)*

Figure 7. SEM micrograph of activated carbon from African pear seed before (7a), after adsorption (7b)

After adsorption, the “After” micrograph showed noticeable changes in surface texture. The particles appeared more agglomerated. These morphological shifts suggest that sulfidic gas molecules were successfully captured and retained on the carbon surface. Such transformations are consistent with previous SEM-based studies on agricultural waste-derived activated carbon used for gas purification [12]. The porous nature of activated carbon is essential for trapping gas molecules. The initial SEM image confirmed the presence of micro- and mesopores, which facilitate the diffusion and retention of acid gases like hydrogen sulfide (H_2S). Post-adsorption, the reduced visibility of these pores implies saturation or coverage by adsorbed compounds, validating the material’s adsorption performance [14].

TheXRDof activated carbon from African pear seed before and after gas capture is shown in Figure 8. The XRD pattern recorded before gas capture shows a dominant, broad reflection around 27.9° 2θ, with smaller humps near 41° and 60.8°. Such a pattern confirms that the activated carbon derived from African pear seeds possesses an amorphous structure with limited graphitic ordering. This structural nature is common in biomass-derived carbons, which usually exhibit high defect densities and abundant surface sites beneficial for adsorption [15].

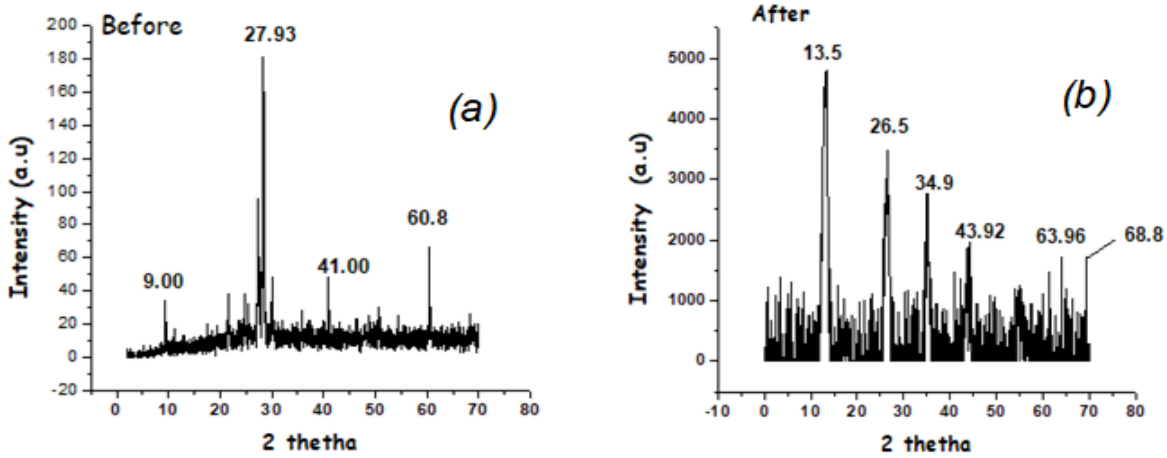

Figure 8. XRD spectrum of activated carbon from African pear seed before (8a) and after (8b) adsorption.

This amorphous microstructure is advantageous for adsorption processes because it enhances surface area, pore accessibility, and the availability of oxygenated functional groups. After H_2S exposure, the XRD pattern changes drastically, with sharp, intense peaks appearing at 13.5°, 26.5°, 34.9°, 43.9°, 63.9°, and 68.8° 2θ, alongside an increase in intensity. This transformation signifies the formation of new crystalline phases within the carbon structure. In H_2S adsorption systems, such crystallization usually results from the chemical conversion of H_2S into solid products like elemental sulfur, metal sulfides, or sulfates on the carbon surface [16]. These phases are formed as H_2S reacts with surface oxygen groups or catalytic metal residues, leading to the deposition of crystalline sulfur or related compounds. The observed increase in intensity indicates a significant buildup of such crystalline products, confirming effective gas capture.

Table 1 showed theBET informationof activated carbon from African pear seed. TheBET analysis is a critical tool for evaluating the surface properties of porous materials, especially in adsorption studies. In this context, activated carbon derived from African pear seeds (*Dacryodes edulis*) was assessed before and after exposure to sulfidic gas.

Table 1. Surface area, pore volume and average diameter of activated carbon from African pear seed

Materials	Surface area (m^2/g)	Total pore volume (cm^3/g)	The pore’s average diameter (nm)
Activated carbon before gas capture	965.200	0.60350	2.40
Activated carbon after gas capture	999.900	0.63548	3.00

The results show an increase in surface area from 965.200 m^2/g to 999.900 m^2/g, total pore volume from 0.60350 cm^3/g to 0.63548 cm^3/g, and average pore diameter from 2.40 nm to 3.00 nm. These changes suggest that the activated carbon underwent structural modifications during gas

adsorption, enhancing its capacity for capturing acid gases. Reports from[17,18] revealed that biomass-derived activated carbons where surface modification and pore development occur during adsorption or gas-solid interactions, leading to improved pore accessibility and slight increases in BET surface area. In addition, adsorption-induced structural changes in porous materials have been shown to alter the internal surface structure and adsorption properties due to molecular interactions with the adsorbent framework [19].

3,2, Adsorption-desorption plots before and after gas capture

Figure 9, presentes the Nitrogen Adsorption-desorption isotherm for activated carbon before and after sulfidic gas capture. The isotherms of nitrogen adsorption and desorption discussed on the activated carbon prior to and after the exposure to sulfidic gases reveal that the adsorption profile was generally similar, meaning that the porous structure of the material remained mostly similar to the adsorption profile. In the first sample, the isotherm shows that nitrogen uptake increases slowly at low levels of relative pressure (P/P_0) typically of microporous materials, then steeper at higher relative pressures that represents the influence of mesopores. The isotherm does not alter its overall shape after exposure to gas, however, exhibits a higher nitrogen adsorption both at moderate and high relative pressure, along with a slightly larger hysteresis loop. This tendency indicates that the sulfidic gases could have interacted with the surface of the activated carbon to result in slight structural rearrangement or expansion of the pores to allow nitrogen to become more accessible to certain pores in the process of BET measurement. Notably, adsorption-desorption curves do not display serious pore blockage, or collapse, but the curves demonstrate that the pore network is kept intact with slightly increased adsorption capacity.

Thus, the post-adsorption isotherm is in agreement with the modest rise of the BET surface area and the pore volume observed in the manuscript, but the variation is small and could be due to minor restructuring of the pores or to a better accessibility of the pores and not a radical increase in new surface area.

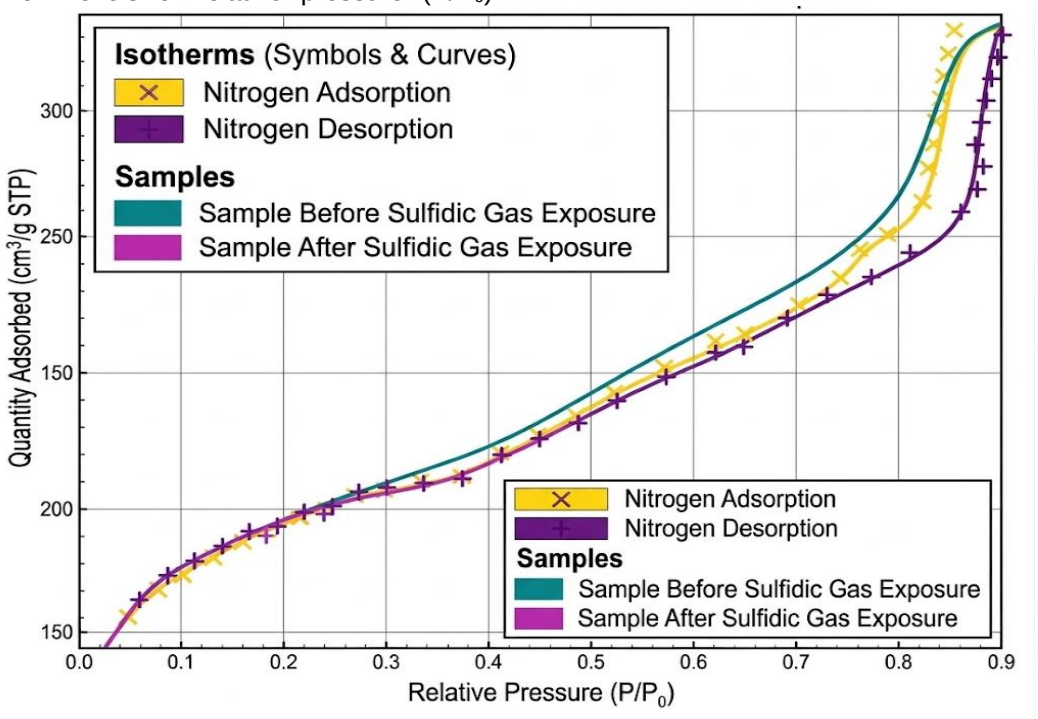

Figure 9. Nitrogen Adsorption-desorption Isotherm for activated carbon before and after sulfidic gas capture

3.3. pHof activated carbon from African pear seed before and after gas capture.

Table 2 presents thepHof activated carbon from African pear seed before and after gascapture. The pH of an adsorbent material is a critical indicator of its surface chemistry and interaction with adsorbates. In this study, the activated carbon derived from *Dacryodes edulis* seeds exhibited a pH of 7.90 before exposure to sulfidic gas, indicating a near-neutral surface. After adsorption, the pH dropped to 6.97, suggesting the uptake of acidic species from the gas stream. This

shift reflects the material's ability to adsorb acid gases such as hydrogen sulfide (H_2S) or sulfur oxides (SO_x). This result, combined with morphological and chemical analyses, reinforces the material's potential for industrial acid gas capture.

Table 2. pH of activated carbon from African pear seed before and after capture

Sample	pH before capture	pH after capture
Activated carbon	7.90	6.97

3.4. Proximate analysis

Table 3 showed themoisture contentof activated carbon from African pear seed before and after gas capture. Moisture content is a critical parameter in evaluating the adsorption behavior of activated carbon, especially when targeting acid gases like hydrogen sulfide (H_2S), which often exist in humid environments. In this study, the moisture content of activated carbon derived from *Dacryodes edulis* seeds increased from 14.7% before to 19.6% after exposure to sulfidic gas. This rise suggests that the material not only adsorbed the target gas but also retained associated water molecules, which is typical in gas streams containing H_2S [20].

Ash content is a critical parameter in evaluating the inorganic residue left after thermal treatment of biomass-based activated carbon. In this study, the ash content of activated carbon derived from *Dacryodes edulis* seeds increased from 7.1% before to 10% after exposure to sulfidic gas. This rise suggests that inorganic compounds, possibly sulfur-containing residues, were retained on the carbon surface during adsorption. Such an increase is often associated with the successful capture of acid gases and their transformation into stable surface-bound species [21].

Volatile matter in activated carbon refers to the fraction of organic compounds that vaporize when the material is heated, excluding moisture. It is a key indicator of the thermal stability and purity of the carbon structure. In this study, the volatile matter content of activated carbon derived from *Dacryodes edulis* seeds decreased from 4.2% before to 3.5% after sulfidic gas adsorption. This reduction implies that the carbon surface became more stable and less reactive after interacting with the gas stream [22]. The decline in volatile matter may be attributed to the adsorption of sulfidic gases, which can lead to surface reactions that stabilize or transform volatile organic compounds.

Fixed carbon represents the non-volatile, solid carbon content in activated carbon that contributes directly to its adsorption capacity. In this study, activated carbon derived from *Dacryodes edulis* seeds showed a decrease in fixed carbon from 74%before to 66.9% after exposure to sulfidic gas. This reduction suggests that the carbon surface was actively involved in the adsorption process, with some carbon sites potentially reacting with or being masked by the adsorbed gas molecules [23].The decline in fixed carbon is indicative of surface saturation or transformation due to chemical interactions with sulfidic gases such as hydrogen sulfide (H_2S).

Table 3. Volatile matter, Moisture content, Ash content and Fixed carbon of activated carbon from African pear seed.

Sample	(%) Before capture	(%) After capture
Moisture content	14.7	19.6
Ash content	7.1	10
Volatile Matter	4.2	3.5
Fixed Carbon	74	66.9

3.5. Results of batch adsorption experiments

3.5.1. Adsorption capacity of the synthesized activated carbon for sulfidic gases from single-component streams at 25^{o}C

Table 4 with graphical representation in Figure 10 present adsorption capacity of the synthesized activated carbon for sulfidic gases from single-component streams at 25°C.The data obtained from the adsorption of sulfidic gases by activated carbon synthesized from African pear seed at varying pressures (P_1 and P_2) at 25°C demonstrate a clear increase in adsorption capacity as pressure rises. Specifically, the adsorption capacity increases from 0.5502 mmol/g at P_1 = 5psi, P_2 = 3psi to 2.9586 mmol/g at P_1 = 20psi, P_2 = 10psi. This result aligns with classical adsorption theory, where increased pressure leads to higher gas density near the adsorbent surface, enhancing the likelihood of collisions between gas molecules and the activated carbon, thus facilitating greater adsorption [24]. Additionally, as pressure increases, the chemical potential difference between the gas phase and the adsorbed phase drives more molecules into available pores, allowing for better utilization of the adsorbent surface area [25].

Table 4. Adsorption capacity at 25 ^{o}C

S/N	$P_{1\ (psi)}$	$P_{2\ (psi)}$	Adsorption capacity (mmol/g)
1	5	3	0.5502
2	10	4	1.1936
3	15	7	1.8183
4	20	10	2.9586

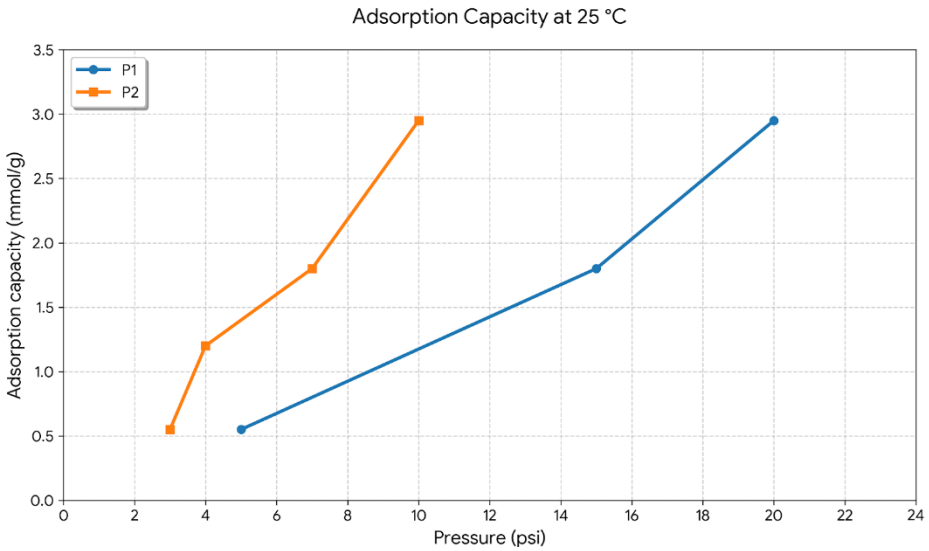

Figure 10. Adsorption capacity of the synthesized activated carbon for sulfidic gases from single-component streamsat 25°C

3.5.2. Adsorption capacity of the synthesized activated carbon for sulfidic gases from single-component streams at 50°C

The adsorption capacity at 50°C is presented in Table 5 and Figure 11, respectively. The adsorption capacity of the activated carbon derived from African pear seed at 50 °C shows a clear increase with rising pressures from P_1 to P_2: from 0.3944 mmol/g at P_1 = 5 psi and P_2 = 2psi, up to 2.1566 mmol/g at P_1 = 20 psi and P_2 = 9.3psi. This progressive rise in uptake reflects the increasing density of sulfidic gas molecules near the adsorbent surface as pressure increases, thereby enhancing the driving force for adsorption and facilitating more collisions and interactions with adsorption sites. Moreover, higher pressures allow more molecules to enter the micropore and mesopore network of the carbon. These trends align with general adsorption theory and empirical findings that show adsorption capacity tends to increase with pressure until pore-filling effects dominate [26].

Table 5. Adsorption capacity at 50 °C

S/N	P_1 (psi)	P2 (psi)	Adsorption capacity (mmol/g)
1	5	2	0.3944
2	10	3.5	1.1927
3	15	5.1	1.5871
4	20	9.3	2.1566

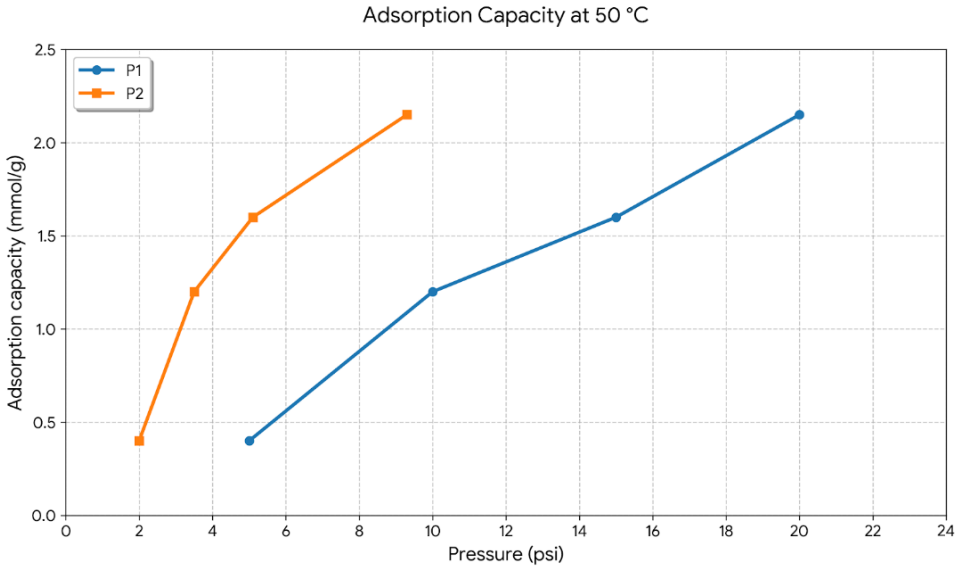

Figure 11. Adsorption capacity of the synthesized activated carbon for sulfidic gases from single-component streams at 50°C

3.5.3. Comparison between adsorption capacity of sulfidic gas at 25°C and 50°C

To compare the adsorption capacity at 25°C and 50°C, the results showed that adsorption is highly temperature-dependent. At lower temperatures (such as 25°C), the adsorption capacity is often higher, as the molecules or ions involved in the adsorption process are more likely to interact with the adsorbent surface. This is because lower temperatures usually result in slower molecular motion, allowing more stable interactions between the adsorbate and the adsorbent. However, at higher temperatures (such as 50°C), the kinetic energy of the molecules increases, leading to a higher rate of desorption and reduced adsorption.

This can cause a decrease in adsorption capacity as the increased thermal energy disrupts the adsorption sites, leading to the release of previously adsorbed molecules. Therefore, the comparison between the two temperatures would likely show a decrease in adsorption capacity at 50°C compared to 25°C, which is typical of physical adsorption processes. However, the specific change in capacity would depend on the nature of the adsorbate (sulfidic gas stream), adsorbent (activated carbon), and the system being studied.

3.5.4. Adsorption capacity of biomass-derived activated carbons for sulfidic gas removal with past literatures

Table 6 presents Comparison of adsorption capacity of biomass-derived activated carbons for sulfidic gas removal in variant with past literatures. In order to put the adsorption performance of the adsorbent synthesized in context, the adsorption capacity achieved in this study (2.96 mmol g^{-1} at 25 ^{o}C) was compared with other literature values of adsorption capacity on the adsorbent obtained using biomass. It has been reported in all literature that the normal adsorption capacities of the conventional activated carbons towards H_2S is usually 0.5-2.0 mmol g^{-1} at ambient temperatures, which varies depending on pore structure, surface chemistry and activation procedure. Corncob, coffee residue, and digestate-derived carbons are also some biomass-derived activated carbons with adsorption capacities of between 1.0 and 2.3 mmol g^{-1}, and modified or composite carbons can achieve slightly higher values.

Table 6. Comparison of adsorption capacity of biomass-derived activated carbons for sulfidic gas removal with past literatures

Adsorbent precursor	Activation method	Adsorbate	Adsorption capacity (mmol g^{-1})	Reference
African pear seed activated carbon	NaOH chemical activation	H_2S/SO_2	2.96	This study
Solid fibrous digestate activated carbon	Physical/chemical activation	H_2S	1.10 - 2.30	[27]
Corncob-derived activated carbon	Chemical activation	H_2S	1.38	[28]
Coffee-residue activated carbon	Cu-impregnated activation	H_2S	1.20	[29]
Agricultural waste activated carbon	Chemical activation	H_2S	0.50 - 2.00	[30]
Aloe-vera biomass carbon	Composite activated carbon	H_2S	3.11	[28]

The adsorption capacity determined of the activated carbon produced out of the African pear seed (2.96 mmol g^{-1}) is thus favourable against most of the adsorbents in literature that have been produced through biomass. This is relatively high performance due to the large BET surface area, well-developed pore structure and presence of surface functional groups that improve the interaction between sulfidic gas molecules and that of the adsorbent surface.

3.6. Adsorption Isotherms

Experimental adsorption data used to generate Langmuir, Freundlich, and Temkin isotherm models for activated carbon derived from African pear seed at 25 ^{o}C and 50 ^{o}C are shown in Figure 12and 13, respectively

3.6.1. Langmuir, Freundlich and Temkin Isotherm at 25 ^{o}C

Figure 12 shows the Langmuir, Freundlich, and Temkin adsorption isotherm models for sulfidic gases on African pear seed-derived activated carbon at 25 ^{o}C. The Langmuir model yielded a low R^2 (0.367), indicating that monolayer adsorption on a homogeneous surface does not adequately describe the process [31]. In contrast, the Freundlich isotherm provided a much better fit with

an R^2 of 0.942. This supports multilayer adsorption on a heterogeneous surface. The Freundlich constant n = 0.784 also confirms favourable adsorption, as n values between 0 and 1 indicate strong interactions between the adsorbate and adsorbent [32, 33].

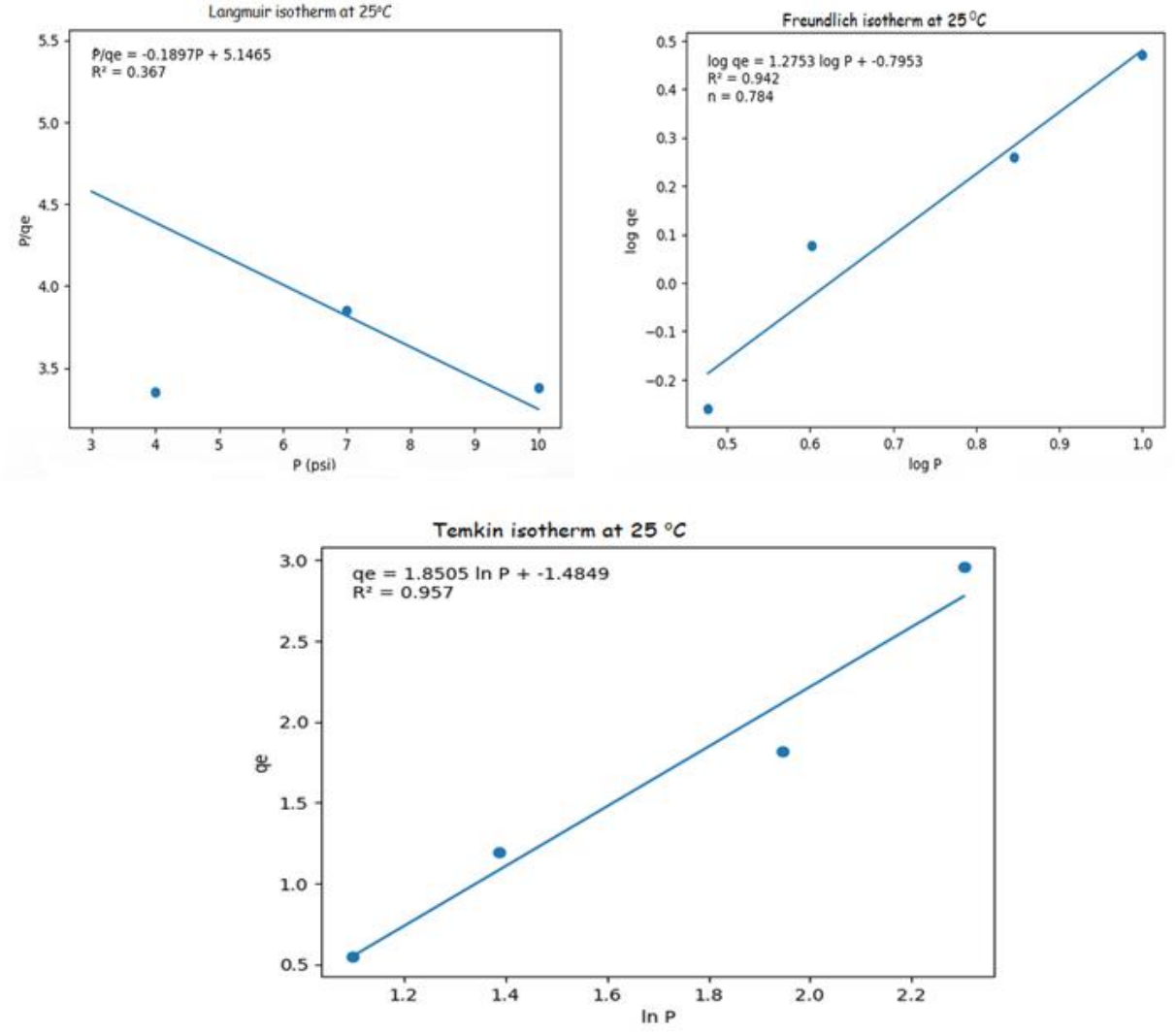

Figure 12. Langmuir, Freundlich, and Temkin isotherm models of activated carbon for sulfidic gases at 25°C

The Temkin isotherm provided the best fit (R^2 = 0.957), making it the most accurate model for describing adsorption equilibrium at 25 °C. This model assumes a linear decrease in the heat of adsorption with increasing surface coverage due to adsorbate-adsorbent interactions [34]. The superior performance of the Freundlich and Temkin models over Langmuir is consistent with literature on biomass-derived activated carbons [35], and reflects the heterogeneous surface nature of the prepared carbon and intermolecular interactions among adsorbed molecules.

3.6.2. Langmuir, Freundlich and Temkin Isotherm at 50 °C

Figure 13 presents the Langmuir, Freundlich, and Temkin isotherm models for sulfidic gas adsorption on African pear seed activated carbon at 50 °C. The Langmuir model gave a very low R^2 (0.001), ruling out monolayer adsorption on a homogeneous surface. The Freundlich model fit significantly better (R^2 = 0.887), with n = 0.927 confirming favourable multilayer adsorption on a heterogeneous surface [34, 35].

The Temkin isotherm achieved the best fit (R^2 = 0.988), indicating that adsorbate–adsorbate interactions significantly influence the adsorption process [36]. The superior R^2 values of both the Freundlich and Temkin models confirm that adsorption occurs on a heterogeneous surface, consistent with findings for biomass-derived activated carbons [37].

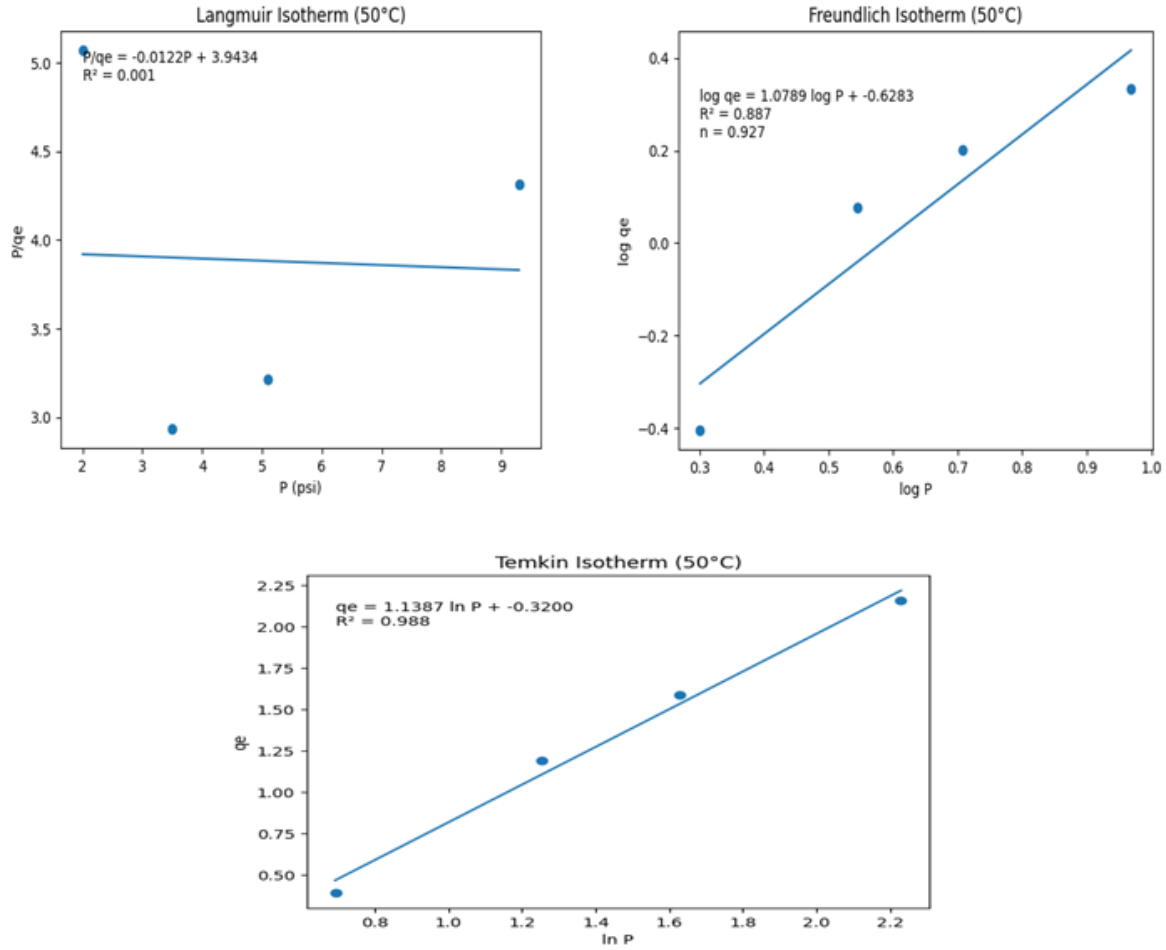

Figure 13. Langmuir, Freundlich, and Temkin isotherm models of activated carbon for sulfidic gases at 50°C

3.7. Statistical Analysis

To determine the reliability and variability of the adsorption capacity data, statistical analysis was performed at 25 °C and 50 °C. As seen in Table 7, the average adsorption capacity at 25 °C was 1.63 ± 1.03 mmol g^{-1}, which is greater than the result at 50 °C (1.33 ± 0.74 mmol g^{-1}). This finding means that sulfidic gas adsorption on activated carbon is more favourable at low temperatures. The increased adsorption capacity at 25 °C is expected for adsorption behaviour, in which adsorption becomes more favourable with increasing temperature, as lower temperatures promote contact between gas molecules and the adsorbent surface. Conversely, with rising temperature, the kinetic energy of gas molecules also increases, which can cause desorption and reduce adsorption efficiency.

The standard deviation is 1.026 mmol g^{-1} at 25 °C and 0.740 mmol g^{-1} at 50 °C, indicating that the adsorption data varies moderately across the different pressure conditions studied. The adsorption capacity also varied more at 25 °C (2.41 mmol g^{-1}) than at 50 °C (1.76 mmol g^{-1}), further confirming the more strongly pressure-dependent adsorption behaviour at lower temperature. In general, the statistical analysis shows that the adsorption results can be reproduced, and indicates that adsorption of sulfidic gases on the synthesised activated carbon is temperature-dependent and more effective at low temperatures.

Table 7. Statistical summary of adsorption capacity at 25 °C and 50 °C

Temp.	n	Mean adsorption capacity (mmol g^{-1})	Standard deviation	Variance	Standard error	Min.	Max.	Range	95% Confidence interval
25 °C	4	1.630	1.026	1.052	0.513	0.550	2.959	2.408	-0.002 - 3.263
50 °C	4	1.333	0.740	0.548	0.370	0.394	2.157	1.762	- 2.510

4. CONCLUSION

This study synthesised and assessed activated carbon from African pear seeds for adsorption of sulfidic gases. The characterisation data showed that the prepared activated carbon had good physicochemical characteristics, including a high surface area, a well-developed pore structure, and active surface functional groups conducive to gas adsorption. FTIR, SEM, EDX, and XRD structural characterisation revealed a high level of surface interactions between the adsorbent and sulfidic gases, including the formation of sulfur-containing surface species and morphological changes upon adsorption. As indicated in the BET analysis, there was a slight increase in surface area and pore volume under gas exposure, suggesting that the pores may have been restructured and that more adsorption sites were exposed.

The adsorption experiments showed that pressure enhanced the adsorption capacity, and the temperature (25 ^{o}C) enhanced the adsorption capacity compared to 50 ^{o}C, which implies that adsorption was affected by temperature and concentration and adsorption was favoured at lower temperatures. The 2.96 mmol g-1 maximum adsorption capacity achieved at 25 °C is comparable to that of most biomass-derived activated carbons reported in the literature. Isotherm modelling showed that the adsorption process followed the Freundlich and Temkin behaviour. This indicates that adsorption is heterogeneous and involves interactions among the adsorbed molecules. Overall, the results indicate that the activated carbon prepared from African pear seeds is an effective, and sustainable adsorbent for the removal of hydrogen sulfide and sulfur dioxide from industrial gas streams, and can be used for gas purification and environmental restoration.

Acknowledgement

The authors appreciates Mr. Akpeji Bamidele Honesty from the Department of Science Laboratory Technology at the Federal University of Petroleum Resources, Effurun, for his valuable help and support during the laboratory analysis in this study.

5. REFERENCES

[1] W. C. Okologume, D. K. Eyitemi, J. O. Okologume, B. H. Akpeji (2025) Potentiation of activated carbon from cassava peels for adsorption of hydrogen sulfide from petroleum streams, *Eur. J. Appl. Sci. Eng. Technol.*, 3 (4), 256–268. https://doi.org/10.59324/ejaset.2025.3(4).21

[2] L. Paz, S. Gentil, V. Fierro, A. Celzard (2025) Activated carbons outperform other sorbents for biogas desulfurization, *Chem. Eng. J.*, 506, 160304. https://doi.org/10.1016/j.cej.2025.160304.

[3] G. Zeng, H. Li, W. Zhang, J. Zhao, L. Wang (2024) Experimental study on adsorption of SO_2 and NH_3 by activated carbon in a fixed-bed reactor, *ACS Omega*, 9, 12345–12356. https://doi.org/10.1021/acsomega.3c07430.

[4] L. Swana, B. T. Bienvenu, V. T. Jacqueline, L. P. S. Louis (2023) The genus *Dacryodes* Vahl.: Ethnobotany, phytochemistry and pharmacology, *Plants*, 12 (9), 1931. https://doi.org/10.3390/plants12091931.

[5] H. Ene-Obong, E. Okeke, A. Ekwochi-Ugbodu (2019) Variations in the nutrients and bioactive compounds of different accessions of African pear (*Dacryodes edulis*), *J. Food Compos. Anal.*, 82, 103232. https://doi.org/10.1016/j.jfca.2019.103232.

[6] M. L. Nguyen, S. Kim, J. H. Lee (2022) Biomass-based activated carbon from pear seed for industrial applications: A sustainable alternative, *J. Clean. Prod.*, 331, 129832. https://doi.org/10.1016/j.jclepro.2022.129832.

[7] T. Sumathi, G. Alagumuthu (2014) Adsorption studies for arsenic removal using activated *Moringa oleifera*, *Int. J. Chem. Eng.*, 14 (1), 430417. https://doi.org/10.1155/2014/430417.

[8] M. Danish, T. Ahmad (2018) A review on utilization of wood biomass as a sustainable precursor for activated carbon production and application, *Renew. Sustain. Energy Rev.*, 87, 1–21. https://doi.org/10.1016/j.rser.2018.02.003.

[9] O. Benhabiles, L. Merabti, N. Chekir, M. Mellal, S. Aoudj, N. A. Abdeslam, D. Tassalit, S. E. I. Lebouachera (2023) Sustainable activated carbon from agricultural waste: A study on adsorption efficiency, *Sustainability*, 16 (21), 9308. https://doi.org/10.3390/su16219308.

[10] M. E. Acuña Montaño, L. Effting, C. L. B. Guedes, G. G. Carbajal Arizaga, R. M. Giona, P. H. Y. Cordeiro, C. R. T. Tarley, A. Bail (2024) Performance assessment of activated carbon thermally modified with iron in the desulfurization of biogas, *J. Anal. Sci. Technol.*, 15, 20. https://doi.org/10.1186/s40543-024-00432-6.

[11] J. Zhang, C. Duan, X. Huang, M. Meng, Y. Li, H. Huang, H. Wang, M. Yan, X. Tang (2024) A review on research progress and prospects of agricultural waste-based activated carbon, *J. Mater. Sci.*, 59, 5271-5292. https://doi.org/10.1007/s10853-024-09526-3.

[12] S. Kundu, M. S. Hossain, T. Khandaker, M. A. Mia Anik, M. K. Hasan (2024) A comprehensive review of enhanced CO_2 capture using activated carbon derived from biomass feedstock, *RSC Adv.*14 (40), 29693-29736. https://doi.org/10.1039/D4RA04537H.

[13] O.-W. Achaw (2012) A study of the porosity of activated carbons using the scanning electron microscope, *IntechOpen*. 473-490. https://www.intechopen.com/chapters/30949.

[14] S. Biniak, G. Szymański, A. Światkowski (1997) The characterization of activated carbons with oxygen and nitrogen surface groups, *Carbon*. 35 (12), 1799-1810.https://doi.org/10.1016/S0008-6223(97)00096-1.

[15] H. Cruz-Martínez (2023) Adsorption of hydrogen sulfide on activated carbon materials derived from agro-industrial residues, *Materials*, 16 (14), 5119. https://doi.org/10.3390/ma16145119.

[16] A. S. Ahmed, M. Alsultan, A. A.Sabah, G. F. Swiegers (2023) Carbon dioxide adsorption by a high-surface-area activated charcoal. *J. Compos. Sci.*, *7*(5), 179. https://doi.org/10.3390/jcs7050179

[17] C. Kessler, R. Schuldt, S. Emmerling, B. V. Lotsch, J. Kästner, J. Gross, N. Hansen (2022) Influence of layer slipping on adsorption of light gases in covalent organic frameworks: a combined experimental and computational study, *Microporous Mesoporous Mater*., 336, 111796. https://doi.org/10.1016/j.micromeso.2022.111796

[18] I. Karume, S. Bbumba, S. Tewolde, I. Z. T. Mukasa, M. Ntale (2023) Impact of carbonization conditions and adsorbate nature on the performance of activated carbon in water treatment, *BMC Chem.*, 17,162.https://doi.org/10.1186/s13065-023-01091-1.

[19] K. S. Ukanwa, K. Patchigolla, R. Sakrabani, E. Anthony, S. Mandavgane (2019) A review of chemicals to produce activated carbon from agricultural waste biomass, *Sustainability*, 11 (22), 6204. https://doi.org/10.3390/su11226204.

[20] R. Gautam, S. Sahoo (2023) A review on adsorption isotherms and kinetics of CO_2 and various adsorbent pairs suitable for carbon capture and green refrigeration applications, *Sādhanā*, 48 (1). https://doi.org/10.1007/s12046-023-02080-9.

[21] H. Jedli, M. Almonnef, R. Rabhi, M. Mbarek, K. Slimi (2024) Activated carbon as an adsorbent for CO_2 capture: Adsorption, kinetics, and RSM modelling, *ACS Omega*, 9, 2080–2087. https://doi.org/10.1021/acsomega.3c02476.

[22] C. Bläker, J. Muthmann, C. Pasel, D. Bathen (2019) Characterization of activated carbon adsorbents – state of the art and novel approaches, *Chem. Bio. Eng. Rev.*, 6 (3), 145–168. https://doi.org/10.1002/cben.201900008.

[23] M.-K. Seo, J.-H. Joo, S.-H. Kim, H.-J. Kang, J. H. Lee, H.-J. Jeon, S.-J. Park (2024) Recent advances in activated carbon fibers for pollutant removal, *Carbon Lett.*, 35, 21–44. https://doi.org/10.1007/s42823-024-00803-4

[24] T. G. Choleva, D. N. Bikiaris, E. A. Deliyanni, K. Z. Kyzas (2023) Removal of hydrogen sulfide using activated carbon derived from solid fibrous digestate: Adsorption performance and regeneration, *J. Environ. Chem. Eng.*, 11 (3), 109763.https://doi.org/10.1016/j.jece.2023.109763.

[25] M. Baikousi, E. Deliyanni, A. C. Mitropoulos, G. Z. Kyzas, D. N. Bikiaris (2023) Activated carbon composites for hydrogen sulfide removal: Adsorption performance and mechanism, *Environ. Res.*, 216, 114448. https://doi.org/10.1016/j.envres.2022.114448.

[26] J. Wang, Y. Chen, L. Liu, Y. Li (2022) Copper-impregnated activated carbon derived from coffee residue for efficient hydrogen sulfide removal, *J. Environ. Manage.*, 308, 114589. https://doi.org/10.1016/j.jenvman.2022.114589.

[27] M. T. Reza, B. Wirth, J. Mumme (2020) Activated carbon derived from agricultural residues for hydrogen sulfide removal from biogas, *Waste Biomass Valorization*, 11, 3255-3266. https://doi.org/10.1007/s12649-019-00664-3.

[28] T. Aprianti, H. M. Hapsari, D. Y. Permata, S. Aprilyanti, J. Sobey, K. Pham, H. T. Chua(2024) Experimental study of gas adsorption using high-performance activated carbon: Propane adsorption isotherm, *Teknomekanik*, 7 (1), 62-73. https://doi.org/10.24036/teknomekanik.v7i1.28672

[29] F. O. Erdogan (2019) Freundlich, Langmuir, Temkin, DR and Harkins-Jura isotherm studies on the adsorption of CO_2 on various porous adsorbents. *Int. J. Chem. React. Eng.*, 17(5), 20180134. https://doi.org/10.1515/ijcre-2018-0134

[30] I. Yazidi, K. Ziat, N. E. Bardiji, Y. E. Boundati, A. Naji, J. E. Haskouri, M. Saidi (2026) Adsorption Kinetics, Isotherm Models, and Thermodynamics: A Brief Review. *Artif. Intell. Emerging Mater. Transition Green Smart Technol*., 93-105. https://doi.org/10.1007/978-3-031-64150-1_8

[31] A. Işıtan (2025) Sustainable adsorption of amoxicillin and sulfamethoxazole onto activated carbon derived from food and agricultural waste: Isotherm modelling and characterization, *Processes*, 13 (8), 2528. https://doi.org/10.3390/pr13082528

[32]J. Singh, S. Basu, H. Bhunia (2019) Dynamic CO_2 adsorption on activated carbon adsorbents synthesized from polyacrylonitrile (PAN): kinetic and isotherm studies. *Microporous Mesoporous Mater.*, 280, 357-366. https://doi.org/10.1016/j.micromeso.2019.02.031

[33] E. R. Khama, E. Z. Loyibo, W. Okologume, S. T. Ekwueme, C. V. Okafor, N. P. Ohia (2024) Investigation of the performance of activated carbon derived from ripe plantain peels for CO_2 capture: Modelling and optimisation using response surface methodology.*Zastit. Mater*., 65 (2), 258-272. https://doi.org/10.62638/ZasMat1149

[34] D. B. Tanko, W. R. Ahulle, H. F. Chahul, I. M. Saviour (2026) Review of adsorption isotherm models.*Appl. Water Sci.*, 16, 72. https://doi.org/10.1007/s13201-025-02682-0

[35] B. H. Akpeji, T. B. Korede, J. Adedokun (2024) Removal of Mn(II) ions from aqueous solution using silver and titanium dioxide nanoparticles derived from bacterial pigment: Experimental characterization and optimization, *Adv. Ind. Eng. Manage.*, 13 (2), 154–165. https://doi.org/10.7508/alem.02.2024.154.165.

[36] W. P. Uwana, F. T. Pereware, M. O. Kigho, B. H. Akpeji, R. O. Ayomide (2025) Optimization of methylene blue adsorption onto biosorbent from palm kernel shell: A design of experiments (DOE) approach, *J. Eng. Res. Innov. Sci. Dev.*, 3(1), 91–96. https://doi.org/10.61448/jerisd31251.

[37] F. T. Pereware, M. O. Ndubuisi, B. H. Akpeji, D. P. Ovonomo, O. S. Joshua (2025) Adsorptive treatment of abattoir wastewater using biosorbent prepared from *Raphia hookeri* seed, *J. Eng. Res. Innov. Sci. Dev.*, 3 (3), 9–13. https://doi.org/10.61448/jerisd33253

IZVOD

ADSORPCIONI KAPACITET AKTIVNOG UGLJA DOBIJENOG IZ SEMENA AFRIČKE KRUŠKE (*Dacryodes edulis*) ZA HVATANJE SULFIDNIH GASOVA

Ova studija istražuje adsorpcioni kapacitet aktivnog uglja dobijenog iz semena afričke kruške (Dacryodes edulis) za hvatanje sulfidnih gasova. Aktivni ugalj je sintetisan hemijskom aktivacijom pomoću natrijum hidroksida (NaOH) i okarakterisan pre i posle adsorpcije gasa, kako bi se procenio njegov potencijal za industrijsko prečišćavanje gasa. Eksperimenti adsorpcije su sprovedeni u sistemu sa fiksnim slojem na 25°C i 50°C, i pod pritiscima u rasponu od 5 do 20 psi. Rezultati karakterizacije su pokazali da se površina aktivnog uglja povećala sa 965,2 m²/g na 999,9 m²/g nakon izlaganja gasu, a prosečan prečnik pora se proširio sa 2,4 nm na 3,0 nm, što ukazuje na poboljšano iskorišćenje pora tokom procesa adsorpcije. FTIR spektri su pokazali smanjenje hidroksilnih i karbonilnih vrhova, zajedno sa pojavom novih vrhova blizu 1328,66 cm⁻¹, što ukazuje na površinske vrste koje sadrže sumpor. SEM mikrografije su pokazale promene u površinskoj morfologiji, sa aglomeracijom i blokiranim porama, što potvrđuje interakciju ugljenika sa sulfidnim gasovima. XRD analiza je otkrila formiranje kristalnih vrsta sumpora, što ukazuje na hemijske interakcije između adsorbenta i sulfidnih gasova. Rezultati pokazuju da je aktivni ugalj iz semena afričke kruške efikasan adsorbent za sulfidne gasove, sa značajnim promenama u njegovim površinskim svojstvima nakon adsorpcije.
***Ključne reči**: Afrička kruška, adsorpcija, hvatanje, gas, sumpor, aktivni ugalj*

Naučni rad
Rad primljen: 16.02.2026.
Rad prihvaćen: 27.03.2026.

Wilfred Chinedu Okologume : https://orcid.org/0000-0002-6317-8936

Omonigho Famous Ovuakporaye https://orcid.org/0009-0003-2520-8377